Towards conjugated polymers with low exciton binding energy

Zhou, Difei

Chapter 5

On the influence of donor-acceptor cross conjugation of conjugated polymers upon charge generation in polymer photovoltaics*

ABSTRACT Two-dimensional donor-acceptor (D-A) conjugated polymers, where the acceptor segments are configured as pendant groups on the polymer backbone consisting solely of donor moieties, naturally exhibit a character of donor-acceptor cross conjugation. In contrast, in standard alternating donor-acceptor copolymers, there is linear conjugation between the donor and acceptor moieties throughout the backbone. Inherent to such a 2-D configuration is the weak electronic communication between the cross-conjugated donor and acceptor moieties. This promotes a unique possibility where upon photoexcitation, the nature of cross conjugation might enable the formation of weakly-bound excitons, which may further lead to enhanced charge generation. This chapter describes the specific deployment of a 2-D polymer featuring a distinct cross conjugation between the thieno[2,3-*c*]pyrrole-4,6-dione acceptor and the thieno[3,4-*b*]thiophene donor moieties, with thiophene spacers in the backbone. Preliminary evaluation of the external quantum efficiency of the single-component device based on this polymer suggested, to our surprise, that the exciton binding energy is unambiguously higher than that of the typical linearly-conjugated polymers. The experimental observation is supported by extensive quantum chemical calculations on a series of cross- and linear-conjugated dimers. Furthermore, quantum chemical calculations suggest that the higher exciton binding energy of cross-conjugated polymers is most likely related to strong electron localization in their excited state, leading to a shorter hole-electron distance.

*This chapter contributes to the following manuscript (in preparation): D. Zhou, M. A. Izquierdo Morelos, N. Y. Doumon, R. C. Chiechi, R. W. A. Havenith, L. Jan Anton Koster, and J. C. Hummelen, "Evidence for Reduced Exciton-binding Energy for Conjugated Polymers with Enhanced Excited-state Charge Delocalization".

5.1 Introduction

Bulk-heterojunction polymer solar cells (BHJ-PSCs)[1] have undergone remarkable progress in the past two decades, with notable contribution from the research on one-dimensional linear-conjugated alternating donor-acceptor copolymers. In these polymers, the donor and acceptor moieties are configured alternatively *via* linear conjugation.[2,3,4,5] On the other hand, performance progress has also been achieved for BHJ-PSCs based on two-dimensional conjugated polymers, where the acceptors are installed as pendant groups on the donor backbone *via* cross conjugation, as represented by a handful of examples.[6,7,8,9,10,11] In this context, early explorations mostly employed thienylenevinylene side chains in conjunction with polythiophene backbones. In another strategy towards two-dimensional conjugated polymers, triphenylamine units were incorporated into the polymer backbone, taking advantage of the relatively low HOMO and high charge carrier mobility of triphenylamine conjugates. Such a design has endowed the polymer with a decent hole mobility and PV devices with a power conversion efficiency of 4.37% when applied in solar cells in combination with [70]PCBM.[6] In recent years, concurrent with the active research on alternating donor-acceptor copolymers, new 2-D polymers have emerged with better light-harvesting capacity and improved intermolecular packing, continuously enhancing solar cell performances. For example, by systematically investigating the acceptor and side-chain effect, Peng et al. have reported an efficiency of 5.65%, which was attributed to its good light absorption, improved charge carrier mobility and well-defined phases in the photovoltaic blend with [70]PCBM.[11] Note that the available structural designs of 2-D donor-acceptor conjugated polymers have commonly been based on an ethylenic linker between the donor backbone and the pendant acceptor moiety, in order to maximize the planarity of the conjugation system.

Compared to the extensive studies on D-A linear-conjugated polymers from various perspectives, the area of fundamental aspects remains virtually unexplored for two-dimensional D-A cross-conjugated donor polymers. Furthermore, in spite of the substantial optimizations on polymer structures in the past decade, the photovoltaic performance of PSCs based on 2-D polymers was still notably lower than that of linear alternating D-A conjugated counterparts, even when the same donor and acceptor moieties were employed. In this respect, deeper fundamental understanding on the photoelectronic properties of 2-D cross conjugated polymers is highly valuable.

The current chapter describes our investigations of the exciton binding energy characteristics of 2-D donor-acceptor cross-conjugated donor polymers. This work is inspired by some inherent characteristics of donor-acceptor cross-conjugated polymers. With some preliminary examinations *via* quantum chemical calculations on some oligomers comprising of a donor backbone and cross-conjugated pendant acceptors, we found that the HOMO of such oligomers is effectively delocalized along the entire backbone, while the LUMO is localized on the acceptor. Also note that a donor-acceptor

cross conjugation naturally features a weaker D-A electronic communication, in comparison with the linear conjugation counterpart. Based on this premise, an interesting possibility was postulated: upon photoexcitation of such a 2-D polymer, the hole-electron pair of the photo-generated exciton might be more separated, due to an enhanced hole delocalization and consequently its weaker communication with the acceptor part. A more separated hole-electron pair would lead to a lower exciton binding energy, enhancing the efficiency of charge generation. In pursuit of testing this hypothesis, we specifically designed a 2-D polymer (**CC1**, as shown in Scheme 1) featuring distinct cross conjugation between the polythiophene donor backbone and the pendant thieno[2,3-*c*]pyrrole-4,6-dione acceptor moieties, bridged with a thieno[3,4-*b*]thiophene moiety. In virtue of the proven concept that TEG chains increase the dielectric constant of organic materials, which may contribute to enhanced dielectric screening,[12,13] we also installed TEG chains instead of alkyl chains as solubilizing side chains. The initial idea behind the design presented here was to obtain a material with reduced exciton binding energy upon photoexcitation, which should be observable when the polymer is subjected to proper photoelectronic experiments. More specifically, we employ here quantum efficiency experiments on actual single-component PV devices, to initiate a direct study of the exciton binding energy characteristics of our organic material. This protocol is motivated by a consensus, that accessing the electrical gap energy (E_{elec}, also referred to as transport gap) of the subject material is the key to obtain the exciton binding energy (E_b), given $E_b = E_{elec} - E_g$, where the optical gap E_g can be readily determined from absorption spectroscopy measurements. In 1965, Castro *et al*. discovered that high-energy photons could generate, in anthracene crystals, mobile charges by a mechanism characteristic of an intrinsic process,[14] which further enabled them to estimate the conduction band of anthracene. This specific protocol was later applied to the study of excitons in poly(*para*-phenylenevinylene), which yielded an exciton binding energy of 0.9±0.15 eV.[20] Over the years, direct photocurrent generation with high-energy photons has been observed and studied with photoactive materials, from both experimental and theoretical perspectives.[15,16] A systematic study of quantum efficiency on a series of representative conjugated polymers was conducted by Li *et al*. in 2016,[19] where it was confirmed that with increased excitation energy, external quantum efficiency (EQE) spectra of pristine polymer films showed a transition from exciton to free-charge generation. This transition was oberved as a steep increase of EQE when the excitation photon energy reached the electrical gap.

5.2 Results and discussion

Polymer design and synthesis. Within the present design, we utilized thieno[3,4-*b*]thiophene instead of an ethylenic linker as the donor-acceptor bridge. Such consideration not only furnishes the donor-acceptor fragment with good coplanarity, but also readily takes advantage of the thiophene chemistry.

Our choice of the acceptor moiety is based on a pre-evaluation of the frontier orbitals of a series of cross-conjugated monomers based on thieno[3,4-*b*]thiophene (for discussion details, see Chapter 3). The necessity for this pre-evaluation is brought forward by (i) the lack of systematic study on cross-conjugation systems, and (ii) our assumption that D-A cross-conjugation, due to its nature of weak donor-acceptor electronic communication, would probably have a relatively small influence when bandgap optimization is under consideration. To this end, we selected thieno[2,3-*c*]pyrrole-4,6-dione as the acceptor, with some extra concern on the potential synthetic challenge. The structure of the resulting polymer (**CC1**, for synthesis details, see Chapter 4) is shown in Figure 1.

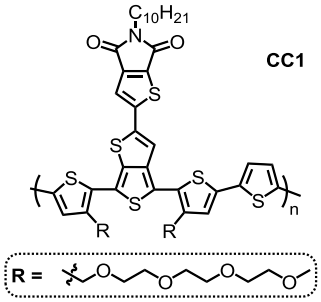

Figure 1. Chemical structure of polymer **CC1**, comprising a polythiophene backbone, thieno[2,3-*c*]pyrrole-4,6-dione acceptor, and a thieno[3,4-*b*]thiophene bridge.

Optoelectronic properties. The UV-vis absorption of **CC1** as a $CHCl_3$ solution is shown in Figure 1(A). Despite our different strategy of using thieno[3,4-*b*]thiophene as the backbone-acceptor linker, the important aspects of the absorption are similar to all previously reported 2-D cross conjugated polymers, i.e., **CC1** showed a notably blue-shifted absorption maximum relative to 1-D donor-acceptor alternating conjugated polymers of similar optical bandgaps, featuring pronounced absorption of the visible photons. The absorption bands peaking at 361 nm and 536 nm are ascribed to the π-π* transition in the pure-donor backbone and the donor-to-acceptor intramolecular charge transfer, respectively.[6,17,18] The thin-film absorption showed a remarkable ~140 nm red shift of the absorption edge relative to that of solution, benefiting from the strong π-π stacking interaction of **CC1** in the solid state.

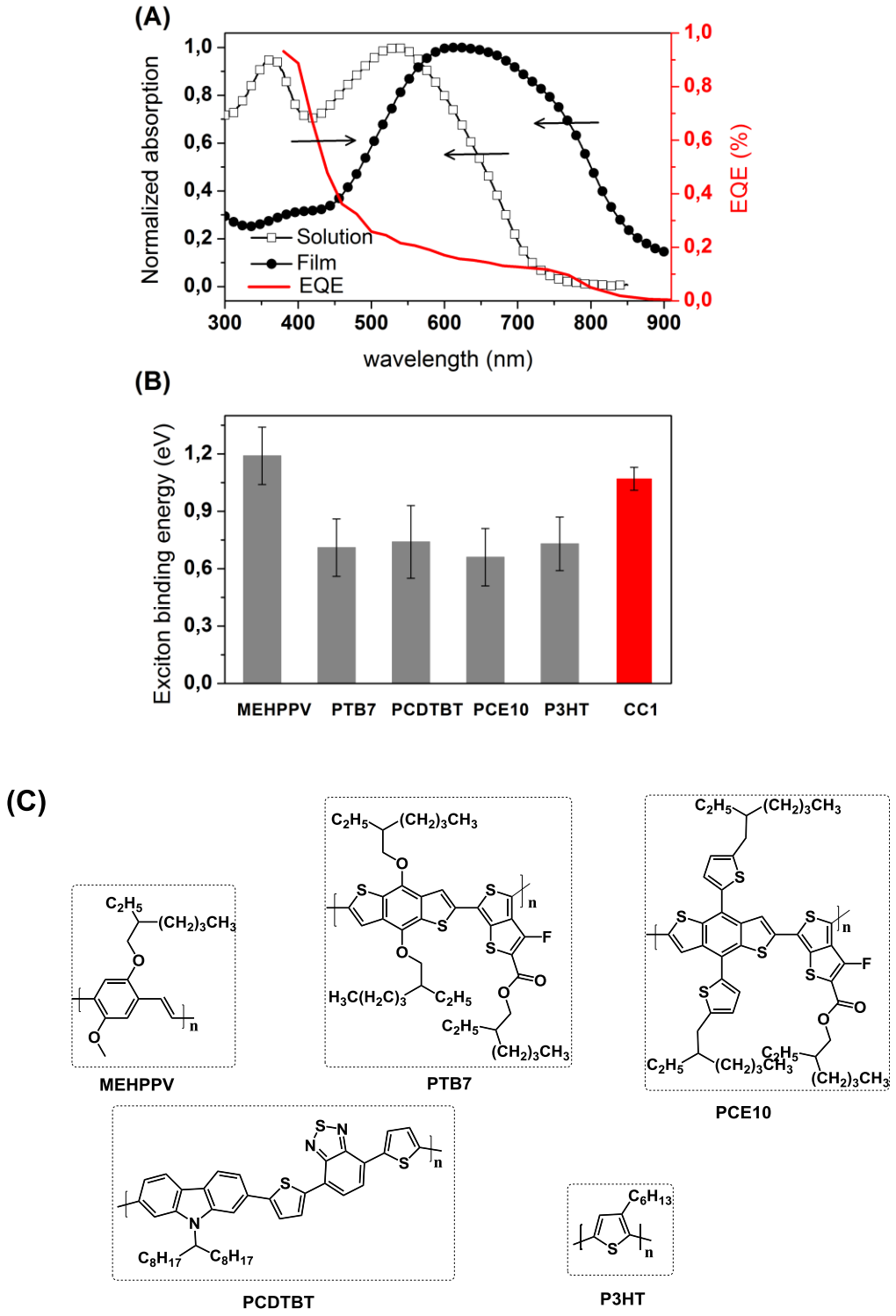

Figure 1. (**A**) Normalized UV-Vis absorption spectra of polymer **CC1** in $CHCl_3$ solution and as a pristine film. The external quantum efficiency of a PV device based on an active layer comprising of solely **CC1** is also included (red curve). (**B**) A bar-chart comparison of exciton-binding energies between **CC1** (red bar) and a few other polymer examples (grey bars) studied elsewhere.[19] The presented exciton binding energies were extracted with the same method. (**C**) The chemical structures of MEHPPV, PTB7, PCDTBT, PCE10 and P3HT.

To validate the initial hypothesis that donor-acceptor cross conjugation may potentially lead to a reduced exciton binding energy upon photoexcitation, we employed the experimental evaluation proposed by Castro[21] and Chandross *et. al*,[20] and developed by Li *et. al*,[19] where the external quantum efficiencies of pristine polymers films are directly used to extract the exciton binding energy.[19,20,21] The EQE profile of a device(ITO/PEDOT:PSS:**CC1**/LiF/Al) with an active layer comprising solely **CC1** is shown in Figure 1(A). The measured EQE starts with an onset at the low-energy side. This onset energy is equal to the optical bandgap of the thin film, confirming the excitation from ground state S_0 to the first singlet excited state S_1. As the photon energy increases, the EQE profile shows a pseudo-plateau region where the EQE values are slightly varied, which corresponds to the excitation to S_1 state and its higher vibrational levels. Note that the flatness of this pseudo-plateau region seems to be related to the intermolecular packing characters of the film, based on our observation on a pseudo-plateau for an as-prepared P3HT film and an actual plateau for an annealed P3HT thin film.

Thin films of pristine **CC1** responded weakly towards thermal annealing. Nevertheless, as the photon energy continues to increase, a clear ~10-fold enhancement of the EQE appeared, the onset of which corresponds to the transport gap.[19] From this, the exciton binding energy was calculated as the interval between the first and second onset. We found a value of 1.07±0.06 eV for **CC1**, with the error based on the statistics of 12 devices. We compared in Figure 1(B) the acquired value to those of a few linearly conjugated D-A polymers and MEHPPV as well as P3HT (as listed in Figure 1(C)). It is worth noting that in spite of the different chemical structures of the presented linearly conjugated polymers, their exciton binding energies seem to be quite close to each other, taking the error bars into consideration. Interestingly, the exciton binding energy of **CC1** is unambiguously higher than most of the other polymers, except MEHPPV. This observation seems to contradict our postulate and it suggests that donor-acceptor cross conjugation in a polymer adversely affects exciton delocalization and dissociation in comparison with linear conjugated polymers. Hence, it would disfavor subsequent charge generation.

Quantum chemical evaluations. The above experimental result indicates that the presented 2-D cross conjugation design does not enhance the photogeneration of free charge carriers, as would be desirable for polymer photovoltaics, caused by a relatively high exciton binding energy of **CC1**. In view of the contrasting observation involving **CC1** and the other representative linearly conjugated polymers, we were inspired to compare and quantify the exciton binding energies of cross-conjugated oligomers and their linearly conjugated counterparts, from a quantum chemical perspective. To do this, we constructed a series of donor-acceptor cross-conjugated oligomers and their linearly conjugated counterparts, as shown in Figure 2(B). Note that the thieno[2,3-*c*]pyrrole-4,6-dione acceptor in **CC1** needs to be transformed into thieno[3,4-*b*]pyrrole-4,6-dione in order to formulate a linear conjugation along the backbone. The exact structures used for the quantum chemical calculations are shown in Figure 2(B). For comparison, we take the vertical exciton binding energy $(E_b^{exc})_{vert}$ as the observable, defined by eq.(1) which is derived in consideration of the reaction $\mathbf{D}^* + \mathbf{D} \rightarrow \mathbf{D}^+ + \mathbf{D}^-$, where $\mathbf{D}^*$, $\mathbf{D}$, $\mathbf{D}^+$ and $\mathbf{D}^-$ refer to the lowest excited-state, ground-state, cation and anion forms of molecule **D**, respectively:

$$(E_b^{exc})_{vert} = E(\mathrm{D}^+) + E(\mathrm{D}^-) - E(\mathrm{D}^*) - E(\mathrm{D}) \qquad (1)$$

where $E(\mathrm{D}^+)$, $E(\mathrm{D}^-)$, $E(\mathrm{D}^*)$ and $E(\mathrm{D})$ represent the total energies of the vertical cationic state, vertical anionic state, vertical first excited state and ground state of the subject molecule. The calculation results of the total energies are included in Table 1, and the exciton binding energies are shown in Figure 2(A).

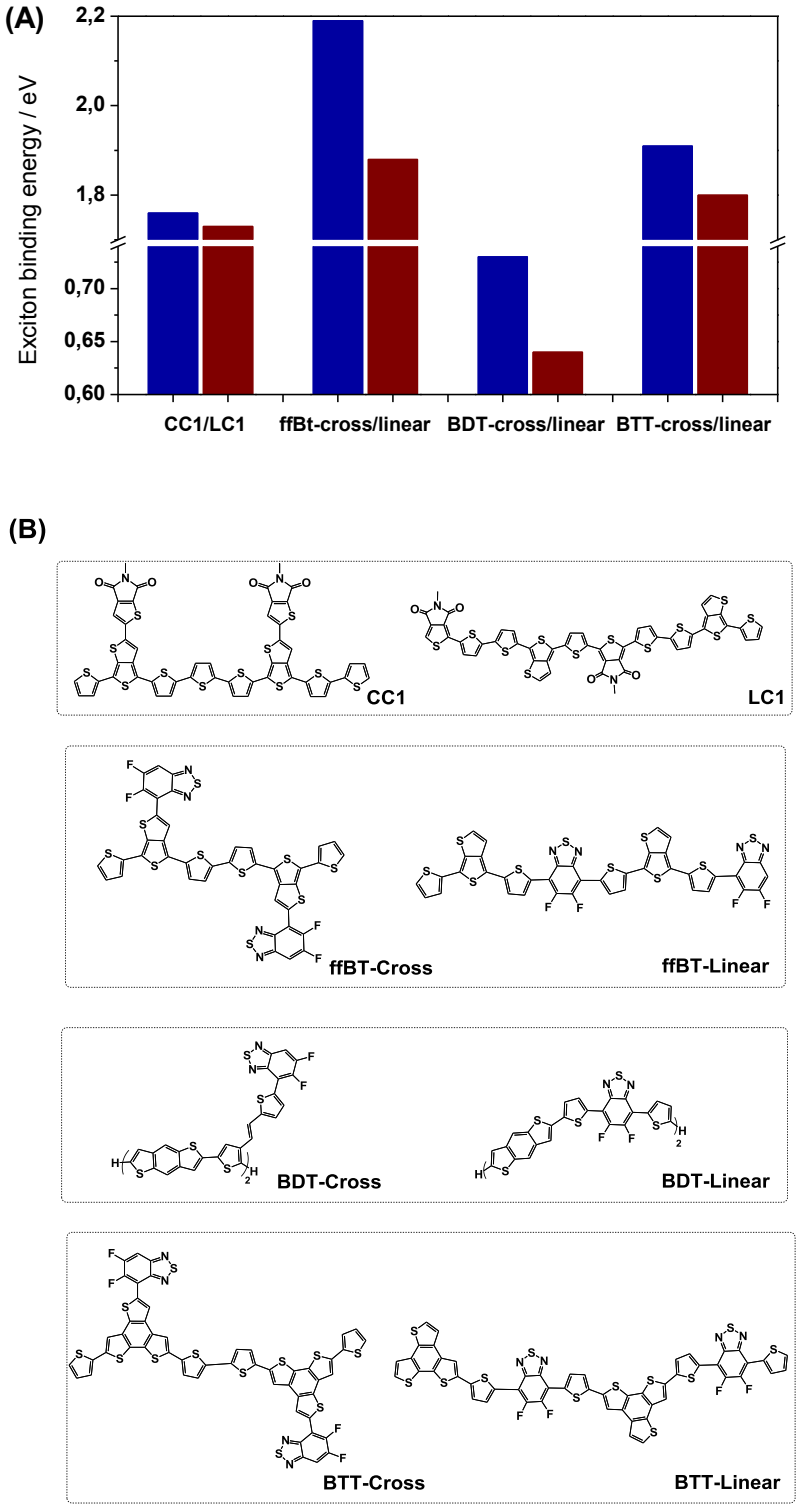

Figure 2. (A) Calculated exciton binding energy comparison of four pairs of cross-conjugated *versus* linear-conjugated dimers. (B) The chemical structures used in the quantum chemical calculations.

Table 1. Calculated total energies of the vertical cationic and anionic states, vertical first excited state and ground state of subject molecules, and deduced exciton binding energies $(E_b^{exc})_{vert}$. For BDT-cross and BDT-linear, total energies of ground-state, vertical cationic and anionic states, charge separated state (E_{cs}) and excited state (E^*) were calculated. Total energies in atomic units. Exciton binding energies were calculated from the total energies and converted to eV (by multiplying 27.211).

structures	$E(D^+)$	$E(D^-)$	$E(D^*)$	$E(D)$	$(E_b^{exc})_{vert}$ (eV)
CC1	–7108.7417	–7109.0453	–7108.8970	–7108.9548	1.76
LC1	–7108.7531	–7109.0498	–7108.9020	–7108.9647	1.73
ffBT-cross	–6133.0972	–6133.4003	–6133.2608	–6133.3109	2.19
ffBT-linear	–6133.0949	–6133.4007	–6133.2547	-6133.3103	1.88
BTT-cross	–7389.6195	–7389.3155	–7389.5356	–7389.4696	1.91
BTT linear	–7389.3083	–7389.6193	–7389.5286	–7389.4654	1.80

structures	$E(D)$	$E(D^+)$	$E(D^-)$	E_{cs}(eV)	E^* (eV)	$(E_b^{exc})_{vert}$(eV)
BDT-cross*	–6593.9478	–6593.7305	–6594.0392	3.4273	2.6940	0.73
BDT-linear*	–6439.2283	–6439.0171	–6439.3305	2.9648	2.3178	0.64

*Energies of BDT-cross and BDT-linear were calculated in a dielectric medium of propanoic acid (dielectric constant $\varepsilon_r \approx 3.5$). Charge separated (CS) states were determined as the difference between the ionization potential of the cation and the electron affinity of the anion in the same configuration as in its respective excited state. Finally, the exciton binding energy was estimated as the difference between E_{cs} and E^*.

In spite of the structure-to-structure difference, and of the qualitative nature of the in-vacuum calculations on dimers, these results tend to suggest that regardless of the donor/acceptor choice and D-A bridging strategies, donor-acceptor cross conjugation results in an increased exciton binding energy compared to the linear conjugation counterpart. While directly correlating the exciton binding energy of organic materials with specific photoelectronic properties remains challenging experimentally, quantum chemical studies can help in understanding the relationship between structure and exciton binding energy in unique perspectives. For example, exciton binding energies of cross- and linear-conjugated molecular systems will be strongly correlated to some of their excited state properties, such as the electron density displacements upon excitation and the subsequent charge separation. To this end, we quantified the charge densities of the ground state and first excited state of a dimer segment from **CC1** (Figure 3(a)) and its linear conjugated counterpart (**LC1**), constructed with the same thiophenic and thienothiophenic units. Herein the construction of a reasonable linear conjugated counterpart is only possible when the thieno[2,3-*c*]pyrrole-4,6-dione moiety in **CC1** is transformed into thieno[3,4-*b*]pyrrole-4,6-dione (Figure 3(c)). We regarded such a transformation viable in consideration of the same

atomic constitution and almost identical electron deficiencies of thieno[2,3-*c*]pyrrole-4,6-dione and thieno[3,4-*b*]pyrrole-4,6-dione.

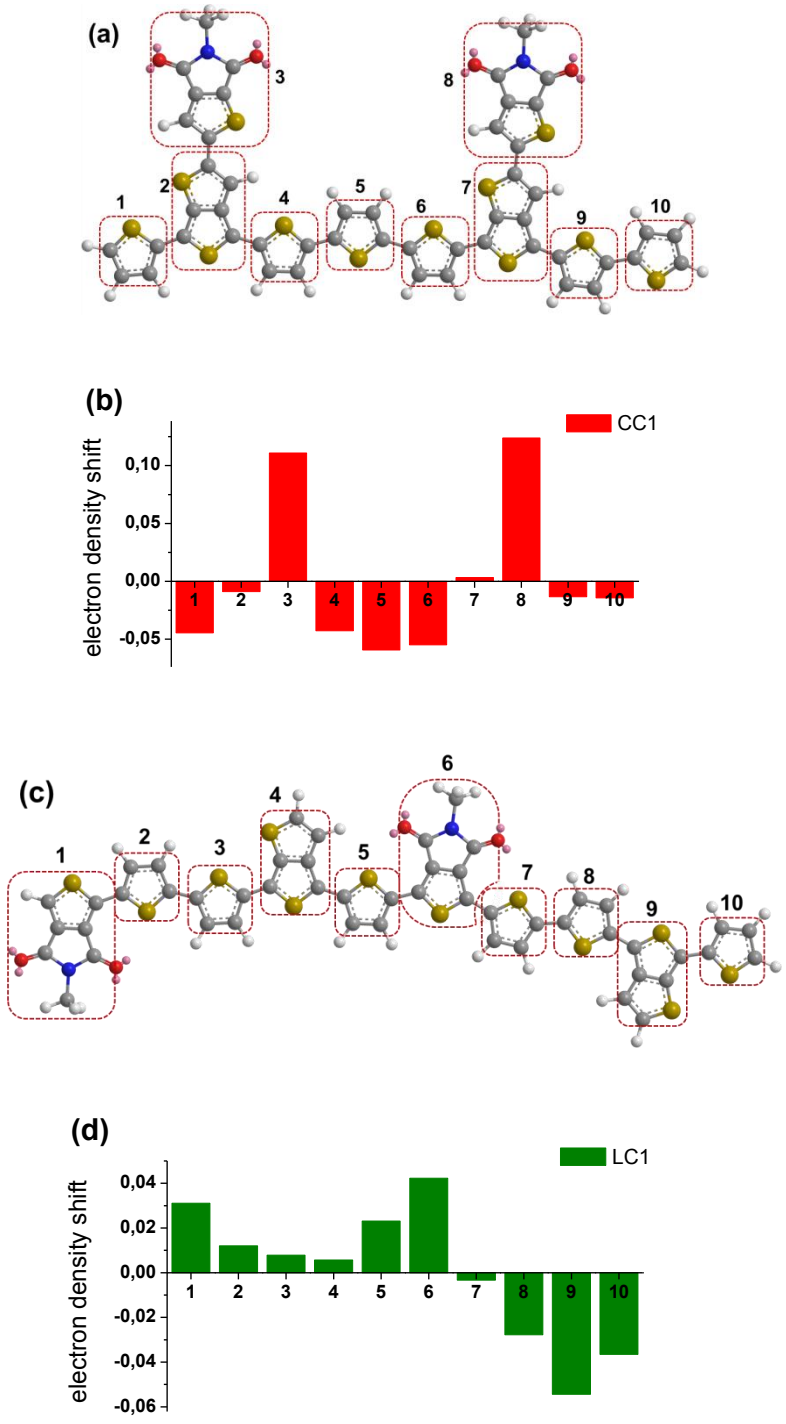

Figure 3. (a) Dimer structure of the building blocks from **CC1**, where the conjugation moieties are numbered from 1 to 10. (b) The electron density shift on each conjugation moiety from ground state to excited state of **CC1**. The numbers in (b) correspond to those in (a). (c) The linear-conjugated counterpart of structure (a), based on the same electron donor and acceptor, named as **LC1** herein. (d) The electron density shift on each conjugation moiety from ground state to excited state of structure (c). The numbers in (d) correspond to those in (c). Note that for both (b)

and (d), a positive value means a gain of electron density and a negative value means a loss of electron density during the excitation process.

The result is visualized by grouping the atoms per conjugation moieties, as shown Figure 3(a) and 3(c), such that each conjugation unit is observed as a contributor to charge displacement upon excitation. For both the cross-conjugated dimer and its linear-conjugated counterpart, there is a noticeable electron transfer from some of the electron-donating moieties to the thienopyrrole-4,6-dione moieties, as clearly indicated by the electron density gains of segments **3** and **8** in Figure 3(b) and segments **1** and **6** in Figure 3(b). A closer look discloses quite different scenarios. In the case of the **CC1** dimer, the electron donation predominantly stems from thiophenic units **4**-**6**, with some extra contribution from unit **1**. Probably due to the weak electronic communication nature of cross conjugation, there is no observable delocalization of electrons, which are almost ubiquitously localized on the small acceptor units. On the other hand, the thienopyrrole-4,6-dione units in the linear conjugated dimer accept electrons from the thiophenic units at the end, suggesting an apparent donor-acceptor character enabled by linear conjugation. A contrasting feature between Figures 3(b) and 3(d) is the notable delocalization of electrons along the conjugation length from segments **1** to **6** in the linear conjugated dimer, arising from efficient electronic coupling involving the thienopyrrole-4,6-dione and thiophenic units. It is noteworthy that our findings are in line with the work by Heeger *et al.*,[22] on a specific linear conjugated donor-acceptor system. There, it was pointed out that despite the strong electron withdrawing capability of the acceptor unit, it does not act solely as an acceptor, but behaves collectively with the neighboring electron-rich moieties as one delocalized segment which might favor photoexciton splitting. Overall, the above analysis implies that good charge delocalization tends to contribute to a lower exciton binding energy, likely benefitting from a spatially more separated hole-electron pair, which is qualitatively shown in Figures 3(b) and 3(d).

5.3 Conclusions

The influence of cross conjugation on the charge generation properties of 2-D conjugated polymers was evaluated experimentally and through quantum chemical calculations. The investigation was conducted by specifically designing a 2-D cross-conjugated thieno[3,4-*b*]thiophene donor/thieno[2,3-*c*]pyrrole-4,6-dione acceptor structure, and further comparing to its linear conjugated counterpart. A few other cross-conjugation/linear-conjugation structures were also compared with the help of quantum chemical calculations. Preliminary evaluation of the external quantum efficiencies of single-component devices suggests that such a 2-D configuration resulted in a relatively high exciton binding energy compared to a series of representative polymers based on linear conjugation throughout the π system. The present study is supported by a quantum chemical comparison of the exciton binding energies of the dimer fragment of the 2-D polymer and a linear conjugated dimer based on the same donor and acceptor moieties. The calculations showed that the 2-D configuration exhibited a higher exciton binding energy relative to the linear configuration. This clearly echoes the above extensive experimental results. The present study does not conclusively indicate a relatively high exciton binding energy for 2-D cross-conjugated polymers, in a universal sense. For that, systematic studies on various structures are necessary to obtain a deeper understanding of this special type of conjugated polymers. In virtue of the currently limited understanding on the fundamental perspectives of 2-D cross conjugated polymers, our study will hopefully contribute to the rational design of conjugated polymers in the future.

5.4 Experimental

Materials and devices. All reagents were purchased from commercial sources and were used without further purification unless indicated otherwise. UV/Vis measurements were conducted on a Perkin Elmer Lambda 9000 spectrometer in 1-cm quartz cuvettes with concentrations of 0.03–0.1 mg/mL in $CHCl_3$. The devices for EQE measurements were fabricated based on indium tin oxide (ITO) coated glass substrates. These substrates were precleaned with deionized water, CMOS grade acetone, and then isopropanol, respectively, each for 15 min. Possible organic residues were removed by UV-ozone cleaning for 20 min. A layer of PEDOT:PSS (poly(3,4-ethylenedioxythiophene):poly(styrenesulfonate), VP AI4083, H. C. Stark) (thickness ~ 60 nm) was spin-cast on top at 1500 rpm for 50 s. After being baked at 140 °C for ~10 min, the substrates were transferred into a nitrogen-filled glovebox (<0.1 ppm of O_2 and H_2O). Atop that polymer solutions were spin-coated in a N_2-filled glovebox from *o*-DCB solution (600 rpm for 5 s and 400 rpm for 120 s). The thickness of the photoactive layers was about 100 nm. Finally, LiF/Al (1 nm and 100 nm, respectively) were thermally evaporated at a pressure of $< 10^{-6}$ Torr on top of the organic layer to make the sandwiched structure ITO/PEDOT:PSS/active layer/LiF/Al.

External quantum efficiency measurements. EQE measurements were performed with a home-built setup equipped with 1000 W Xenon Arc Lamp (Newport) as light source, monochromator (Zolix), optical chopper (ThorLabs), lock-in amplifier (Standard Research SR830), current amplifier (Standard Research SR570), and calibrated Silicon and Germanium detectors (ThorLabs). The beam spot used for EQE measurement was focused and collimated with a set of optical lenses. The EQE spectra were measured at zero bias.

Quantum chemical calculations. Geometries of all structures except BDT-cross/linear were optimized using DFT (B3LYP/6-31G**) with the program GAMESS-UK.[23] Vertical excitation energies were calculated using time-dependent DFT (TD-DFT). The lowest 10 vertical excitation energies were calculated using TD-DFT (B3LYPg/aug-cc-pVDZ) with DALTON.[24] Geometry optimizations and electron densities of BDT-cross/linear were calculated at Density Functional Theory (DFT) level by using the B3LYP exchange correlation functional[25],[26] in combination with the cc-pVDZ basis set as implemented in the Gaussian 09 software package.[27] Lowest singlet excited states were calculated using TD-DFT by using the long-range corrected functional CAM-B3LYP with the cc-pVDZ basis set (also as implemented in Gaussian 09). In the modelling of BDT-cross/linear structures, a polarisable continuum model was used with propanoic acid as the solvent. For a given structure/configuration, local excited states of the dimers were computed and characterized using TD-DFT. The charge density shifts upon excitation were estimated using a Mulliken population analysis of the ground state and excited state densities.

5.5 References

1 G. Yu, J. Gao, J. C. Hummelen, F. Wudl, A. J. Heeger, *Science*, **1995**, 270, 1789.

2 Cheng, Y. J.; Yang, S. H.; Hsu, C. S. *Chem. Rev.* **2009**, *109* (11), 5868–5923.

3 Zhou, H.; Yang, L.; You, W. *Macromolecules* **2012**, *45* (2), 607–632.

4 Roncali, J. *Macromol. Rapid Commun.* **2007**, *28* (17), 1761–1775.

5 Zhao, W.; Li, S.; Yao, H.; Zhang, S.; Zhang, Y.; Yang, B.; Hou, J. *J. Am. Chem. Soc.* **2017**, *139* (21), 7148–7151.

6 Huang, F.; Chen, K.-S.; Yip, H.-L.; Hau, S. K.; Acton, O.; Zhang, Y.; Luo, J.; Jen, A. K.-Y. *J. Am. Chem. Soc.* **2009**, *131* (39), 13886–13887.

7 H. Huang, Z. Cao, Z. Gu, X. Li, B. Zhao, P. Shen, S. Tan, *Eur. Polym. J.*, **2012**, 48, 1805.

8 E. Zhu, J. Hai, Z. Wang, B. Ni, Y. Jiang, L. Bian, F. Zhang, W. Tang, *J. Phys. Chem. C*, **2013**, 117, 24700.

9 H. Tan, X. Deng, J. Yu, B. Zhao, Y. Wang, Y. Liu, W. Zhu, H. Wu, Y. Cao, *Macromolecules*, **2013**, 46, 113.

10 P. Shen, H. Bin, L. Xiao, Y. Li, *Macromolecules*, **2013**, 46, 9575.

11 X. Xu, K. Feng, K. Li, Q. Peng, *J. Mater. Chem. A*, **2015**, 3, 23149.

12 Jahani, F.; Torabi, S.; Chiechi, R. C.; Jan, L.; Koster, A.; Hummelen, J. C. *Chem. Commun.* **2014**, *50*, 1–3

13 Shao, S.; Abdu-Aguye, M.; Qiu, L.; Lai, L.-H.; Liu, J.; Adjokatse, S.; Jahani, F.; Kamminga, M. E.; ten Brink, G. H.; Palstra, T. T. M.; Kooi, B. J.; Hummelen, J. C.; Antonietta Loi, M. *Energy Environ. Sci.* **2016**, *9* (7), 2444–2452.

14 Castro, G.; Hornig, J. F. *J. Chem. Phys.* **1965**, *42* (4), 1459–1460.

15 Petelenz, P.; Mucha, D. *J. Chem. Phys.* **1994**, *100* (6), 4607–4614.

16 Hahn, T.; Tscheuschner, S.; Saller, C.; Strohriegl, P.; Boregowda, P.; Mukhopadhyay, T.; Patil, S.; Neher, D.; Bässler, H.; Köhler, A. *J. Phys. Chem. C* **2016**, *120* (43), 25083–25091.

17 Xu, X.; Feng, K.; Li, K.; Peng, Q. *J. Mater. Chem. A* **2015**, *3* (46), 23149–23161.

18 Tang, W. *J. Phys. Chem. C* **2013**, *117*, 24700–24709.

19 Li, H. W.; Guan, Z.; Cheng, Y.; Lui, T.; Yang, Q.; Lee, C. S.; Chen, S.; Tsang, S. W. *Adv. Electron. Mater.* **2016**, *2* (11), 1600200-1600209.

20 Chandross, M.; Mazumdar, S.; Jeglinski, S.; Wei, X.; Vardeny, Z. V.; Kwock, E. W.; Miller, T. M. *Phys. Rev. B* **1994**, *50* (19), 14702–14705.

21 Castro, G.; Hornig, J. F. *J. Chem. Phys.* **1965**, *42* (4), 1459–1460.

22 Banerji, N.; Gagnon, E.; Morgantini, P. Y.; Valouch, S.; Mohebbi, A. R.; Seo, J. H.; Leclerc, M.; Heeger, A. J. *J. Phys. Chem. C* **2012**, *116* (21), 11456–11469.

23 Guest, M. F.; Bush, I. J.; Van Dam, H. J. J.; Sherwood, P.; Thomas, J. M. H.; Van Lenthe, J. H.; Havenith, R. W. A.; Kendrick, J. *Mol. Phys.* **2005**, *103* (6–8), 719–747.

24 Aidas, K.; Angeli, C.; Bak, K. L.; Bakken, V.; Bast, R.; Boman, L.; Christiansen, O.; Cimiraglia, R.; Coriani, S.; Dahle, P.; Dalskov, E. K.; Ekström, U.; Enevoldsen, T.; Eriksen, J. J.; Ettenhuber, P.; Fernández, B.; Ferrighi, L.; Fliegl, H.; Frediani, L.; Hald, K.; Halkier, A.; Hättig, C.; Heiberg, H.; Helgaker, T.; Hennum, A. C.; Hettema, H.; Hjertenæs, E.; Høst, S.; Høyvik, I. M.; Iozzi, M. F.; Jansík, B.; Jensen, H. J. A.; Jonsson, D.; Jørgensen, P.; Kauczor, J.; Kirpekar, S.; Kjærgaard, T.; Klopper, W.; Knecht, S.; Kobayashi, R.; Koch, H.; Kongsted, J.; Krapp, A.; Kristensen, K.; Ligabue, A.; Lutnæs, O. B.; Melo, J. I.; Mikkelsen, K. V.; Myhre, R. H.; Neiss, C.; Nielsen, C. B.; Norman, P.; Olsen, J.; Olsen, J. M. H.; Osted, A.; Packer, M. J.; Pawlowski, F.; Pedersen, T. B.; Provasi, P. F.; Reine, S.; Rinkevicius, Z.; Ruden, T. A.; Ruud, K.; Rybkin, V. V.; Sałek, P.; Samson, C. C. M.; de Merás, A. S.; Saue, T.; Sauer, S. P. A.; Schimmelpfennig, B.; Sneskov, K.; Steindal, A. H.; Sylvester-Hvid, K. O.; Taylor, P. R.; Teale, A. M.; Tellgren, E. I.; Tew, D. P.; Thorvaldsen, A. J.; Thøgersen, L.; Vahtras, O.; Watson, M. A.; Wilson, D. J. D.; Ziolkowski, M.; Ågren, H. *Wiley Interdiscip. Rev. Comput. Mol. Sci.* **2014**, *4* (3), 269–284.

25 Becke, A. D. *Phys. Rev. A* **1988**, *38* (6), 3098–3100.

26 Lee, C.; Yang, W.; Parr, R. G. *Phys. Rev. B* **1988**, *37* (2), 785–789.

27 Frisch, M. J. E. A., et al. **2009**, *Gaussian 09, revision D. 01*.